

# Anisotropy of the semi-classical gluon field of a large nucleus at high energy

Adrian Dumitru\*

*Department of Natural Sciences, Baruch College, CUNY,  
17 Lexington Avenue, New York, NY 10010, USA and*

*The Graduate School and University Center, The City University of New York, 365 Fifth Avenue, New York, NY 10016, USA*

Vladimir Skokov†

*Department of Physics, Western Michigan University, Kalamazoo, MI 49008, USA*

The McLerran-Venugopalan model describes a highly boosted hadron/nucleus as a sheet of random color charges which source soft classical Weizsäcker-Williams gluon fields. We show that due to fluctuations, individual configurations are azimuthally anisotropic. We present initial evidence that impact parameter dependent small- $x$  JIMWLK resummation preserves such anisotropies over several units of rapidity. Finally, we compute the first four azimuthal Fourier amplitudes of the S-matrix of a fundamental dipole in such background fields.

## I. INTRODUCTION

To explain azimuthal asymmetries observed in high-energy pA collisions [1–5] Refs. [6–8] argued that individual configurations of the light-cone electric fields of the target should be anisotropic, leading to a non-trivial azimuthal distribution of a projectile parton scattered off such a target. That is, configuration by configuration, two-dimensional rotational symmetry is broken by  $\mathbf{E}$ -field “domains” of finite size in the impact parameter plane. These, in contrast to Weiss magnetic domains separated by domain walls, arise purely due to fluctuations of the valence (large- $x$ ) random color charge sources for the soft, small- $x$   $\mathbf{E}$  field.

Assuming such azimuthal anisotropy of the light-cone electric fields several features of the data could be described, at least qualitatively [7, 8]. On the other hand, a direct calculation of the anisotropic distributions, in particular for a large nucleus and small  $x$  (i.e. high energy), has so far been lacking. It is our goal here to compute scattering of a dipole off a large nucleus, and specifically, to determine its angular dependence. That is, we compute the (first four) Fourier amplitudes of the dipole S-matrix with respect to the azimuthal orientation of the dipole. We should stress that we do not address the fluctuations of  $\mathcal{S}(\mathbf{r}, \mathbf{b})$  in impact parameter space  $\mathbf{b}$  (see Ref. [9] for a recent study) but rather its dependence on the size and *orientation* of the dipole vector  $\mathbf{r}$  which is the variable conjugate to the transverse momentum of the parton in the final state.

## II. THE MODEL

In the McLerran-Venugopalan model [10] the large- $x$  valence partons are viewed as random, recoilless color charges  $\rho^a(\mathbf{x})$  which source the semi-classical small- $x$  gluon fields. We first provide a brief description of how these color charge configurations are generated on a lattice; more detailed discussions can be found in the literature [11, 12].

The effective action describing color charge fluctuations is taken to be quadratic,

$$S_{\text{eff}}[\rho^a] = \int dx^- d^2\mathbf{x} \frac{\rho^a(x^-, \mathbf{x}) \rho^a(x^-, \mathbf{x})}{2\mu^2} \quad (1)$$

with  $\mu^2 \sim g^2 A^{1/3}$  proportional to the thickness of a nucleus [10]; here  $A$  denotes the number of nucleons in the nucleus. The variance of color charge fluctuations determines the average saturation scale  $Q_s^2 \sim g^4 \mu^2$  [13]. The coarse-grained effective action (1) applies to (transverse) area elements containing a large number of large- $x$  “valence” charges,  $\mu^2 \Delta A_\perp \sim \Delta A_\perp Q_s^2 / g^4 \gg 1$ .

Hence, in the first step we construct a random configuration of color charges on a lattice according to the distribution

---

\*Electronic address: Adrian.Dumitru@baruch.cuny.edu

†Electronic address: Vladimir.Skokov@wmich.edu

$\exp(-S[\rho])$ . Their (non-Abelian) Weizsäcker-Williams fields are pure gauges; in covariant gauge,

$$A^{\mu a}(x^-, \mathbf{x}) = -\delta^{\mu+} \frac{g}{\nabla^2} \rho^a(x^-, \mathbf{x}) . \quad (2)$$

This also satisfies  $A^- = 0$  and thus the only non-vanishing field strength is  $F^{+i} = -\partial^i A^+$ . The (light-cone) electric field is

$$E^i = \int dx^- F^{+i} = -\partial^i \int dx^- A^+ . \quad (3)$$

The propagation of a fast charge in this field is described by an eikonal phase given by a light-like SU(3) Wilson line  $V(\mathbf{x})$ :

$$V(\mathbf{x}) = \mathbb{P} \exp \left\{ ig^2 \int dx^- \frac{1}{\nabla^2} t^a \rho^a(x^-, \mathbf{x}) \right\} , \quad (4)$$

where  $\mathbb{P}$  denotes path-ordering in  $x^-$ . The absolute value squared of this amplitude gives the S-matrix for scattering of this charge off the given target field configuration,

$$\mathcal{S}_\rho(\mathbf{r}, \mathbf{b}) \equiv \frac{1}{N_c} \text{tr} V^\dagger(\mathbf{x}) V(\mathbf{y}) , \quad \mathbf{r} \equiv \mathbf{x} - \mathbf{y} , \quad 2\mathbf{b} \equiv \mathbf{x} + \mathbf{y} . \quad (5)$$

Thus, following the ideas leading to the MV model we assume that every particular scattering event probes one particular configuration in the target, i.e. that the S-matrix is computed with a frozen  $\rho^a(\mathbf{x})$ . The main purpose of this paper is to analyze the dependence of the S-matrix on the angular orientation of the dipole vector  $\mathbf{r}$ , conjugate to the transverse momentum, at fixed transverse impact parameter (coordinate)  $\mathbf{b}$ .

The S-matrix for a fundamental charge is complex (for three or more colors). Its real (imaginary) part corresponds to  $\mathcal{C}$ -even ( $\mathcal{C}$ -odd) exchanges [14]:

$$1 - D_\rho(\mathbf{r}) \equiv \text{Re} \mathcal{S}_\rho(\mathbf{r}) = \frac{1}{2N_c} \text{tr} [V^\dagger(\mathbf{x}) V(\mathbf{y}) + V^\dagger(\mathbf{y}) V(\mathbf{x})] , \quad (6)$$

$$O_\rho(\mathbf{r}) \equiv \text{Im} \mathcal{S}_\rho(\mathbf{r}) = \frac{-i}{2N_c} \text{tr} [V^\dagger(\mathbf{x}) V(\mathbf{y}) - V^\dagger(\mathbf{y}) V(\mathbf{x})] . \quad (7)$$

$\mathcal{C}$  conjugation transforms  $\rho^a(\mathbf{x}) \rightarrow -\rho^a(\mathbf{x})$  and  $V(\mathbf{x}) \rightarrow V^*(\mathbf{x})$ . The dipole scattering amplitude  $D_\rho(\mathbf{r}) = D_\rho(-\mathbf{r})$  is even under  $\mathbf{r} \rightarrow -\mathbf{r}$  and generates even azimuthal  $v_{2n}$  harmonics while the odderon  $O_\rho(\mathbf{r}) = -O_\rho(-\mathbf{r})$  generates odd  $v_{2n+1}$  [7] of the one-particle distribution.

It is useful to consider the limit of small dipoles,  $rQ_s \ll 1$ . Then the real part of the S-matrix from Eq. (6) is

$$\text{Re} \mathcal{S}_\rho(\mathbf{r}) - 1 = \frac{(ig)^2}{2N_c} \text{tr} (\mathbf{r} \cdot \mathbf{E})^2 + \mathcal{O}(r^4) . \quad (8)$$

To compute the elliptic (dipole) asymmetry, Refs. [6–8] considered the following angular dependence of the two-point function

$$\frac{g^2}{2N_c} \langle \text{tr} E^i(\mathbf{b}_1) E^j(\mathbf{b}_2) \rangle = \frac{1}{4} Q_s^2 \Delta(\mathbf{b}_1 - \mathbf{b}_2) \left( \delta^{ij} + 2\mathcal{A} \left( \hat{a}^i \hat{a}^j - \frac{1}{2} \delta^{ij} \right) \right) , \quad (9)$$

where  $\hat{\mathbf{a}}$  corresponds to the “event plane” orientation, and  $\Delta(\mathbf{b}_1 - \mathbf{b}_2)$  describes the  $\mathbf{E}$ -field correlations in the transverse impact parameter plane. It is implicit that for each configuration  $\mathbf{E}(\mathbf{b})$  is rotated to point in a particular, fixed direction  $\hat{\mathbf{a}}$  before performing the ensemble average. In fact, Eq. (9) is the MV model analogue of the gluon TMD for an unpolarized target [15, 16],

$$\delta^{ij} f_1^g(x, \mathbf{k}^2) + \left( \hat{k}^i \hat{k}^j - \frac{1}{2} \delta^{ij} \right) h_1^{\perp g}(x, \mathbf{k}^2) . \quad (10)$$

Thus, the amplitude  $\mathcal{A}$  from Eq. (9), which we shall denote  $A_2(r)$  below, is basically  $h_1^{\perp g}$  at small  $x$ . However, beyond the MV model the relation between these functions may be more involved.

The action (1) is  $\mathcal{C}$ -even and so  $\langle O_\rho(\mathbf{r}) \rangle = 0$  while  $\langle D_\rho(\mathbf{r}) \rangle \sim r^2 Q_s^2$  (at small  $r$ ) is proportional to the thickness of the nucleus,  $A^{1/3}$ . A  $\mathcal{C}$ -odd operator

$$\frac{1}{\kappa_3} d^{abc} \rho^a \rho^b \rho^c \quad (11)$$

with  $\kappa_3 \sim g^3 A^{2/3}$  could be added to the action<sup>1</sup> which would then induce an expectation value  $\sim A^{1/3}$  for the odderon [17]. This is beyond the scope of the present paper, we focus here on azimuthal anisotropies due to fluctuations of the charge densities  $\rho^a(\mathbf{x})$  and their associated electric fields  $\mathbf{E}^a(\mathbf{x})$ . The main point is that even though the ensemble averaged S-matrix is isotropic and real (even under charge conjugation) that fluctuations generate anisotropies and C-odd contributions locally in impact parameter space for individual configurations.

### III. IMPLEMENTATION

To generate the random configurations  $\rho^a(x^-, \mathbf{x})$  via Monte-Carlo techniques we discretize the longitudinal and transverse coordinates. The number of sites in the longitudinal direction is taken to be  $N_- = 100$  while the number of sites in either transverse direction is  $N_\perp = 1024$ . All of our results presented here have been obtained with  $g^2 \mu a = 0.05$ , hence  $g^2 \mu L = 51.2$ , where  $a \equiv L/N_\perp$  denotes the transverse lattice spacing. We have determined numerically that  $Q_s \approx 0.7125 g^2 \mu$  as defined from

$$\langle \mathcal{S}_\rho \rangle(r = \sqrt{2}/Q_s) = \exp(-1/2). \quad (12)$$

The physical value for the lattice spacing could be determined by assigning a physical value to  $Q_s$ ; instead, we choose to measure distance scales in units of  $1/Q_s$  or  $1/g^2 \mu$  and so this step is not required.

We use periodic boundary conditions in the transverse directions and solve the Poisson equation (2) by Fast Fourier Transform. The amplitude of the zero mode of  $\rho^a(\mathbf{k})$  is set to zero before inversion which ensures color neutrality of each configuration. Alternatively, one could introduce a mass cutoff  $m \ll Q_s$  in the Coulomb propagator in eq. (2). Either way, the dynamics of modes with  $k$  well above the IR cutoff is the same.

We have generated about  $10^4$  configurations; for each of them we measured  $D_\rho(\mathbf{r})$  and  $O(\mathbf{r})$  at  $\mathbf{b} = 0$ . Both functions were decomposed into their Fourier series to extract the amplitudes of azimuthal anisotropy:

$$D_\rho(\mathbf{r}) = \mathcal{N}(r) \left( 1 + \sum_{n=1}^{\infty} A'_{2n}(r) \cos(2n\phi_r) \right), \quad (13)$$

$$O_\rho(\mathbf{r}) = \mathcal{N}(r) \sum_{n=0}^{\infty} A'_{2n+1}(r) \cos((2n+1)\phi_r). \quad (14)$$

The function  $\mathcal{N}(r)$  is the isotropic part of the dipole S-matrix, see for example Ref. [12]. For a small dipole,  $\langle \mathcal{N} \rangle(r) \sim \frac{1}{4} r^2 Q_s^2$ , up to logarithms.

The S-matrix  $\mathcal{S}_\rho(\mathbf{r})$  rotates randomly from configuration to configuration. This manifests as a random shift  $\phi_r \rightarrow \phi_r - \psi$  in eqs. (13,14). Hence, on average over all configurations  $\langle A'_n \rangle = 0$  for all  $n$ . This is a consequence of the fact, already mentioned above, that the ensemble average of the S-matrix is real and isotropic.

Azimuthal harmonics  $v_n$  in hadronic collisions are defined from multi-particle correlation functions in such a way that they are invariant under a global shift of the azimuthal angles of all particles by the same amount. Consequently, we discard this random phase by defining  $A_n = \frac{\pi}{2} |A'_n|$ ; the factor of  $\pi/2$  arises as the inverse average of  $\int d\Delta\phi/(2\pi) |\cos n\Delta\phi| = 2/\pi$ . In other words, we define the amplitudes  $A_n$  such that fluctuations do not average out. We finally obtain their expectation values over the ensemble of configurations,  $\langle A_1 \rangle, \dots, \langle A_4 \rangle$ , as well as the variances of  $A_1$  and  $A_2$ .

### IV. RESULTS

Before presenting our results for the azimuthal amplitudes we show two examples for  $\mathcal{S}_\rho(\mathbf{r})$  in Figs. 1 and 2. Either of these corresponds to one particular (random) configuration of color charges. The real parts display predominantly a  $\sim \cos(2\phi)$  angular dependence, with  $\phi$  the angle between  $\mathbf{r}$  and  $\mathbf{E}(\mathbf{b} = 0)$ . On the other hand, the imaginary part for the configuration shown in Fig. 1 is predominantly  $\sim \cos(\phi)$  while that from Fig. 2 is mainly  $\sim \cos(3\phi)$ , modulo a random phase shift as mentioned above. The figures show, also, that the angular structures appear at a resolution on the order of  $r g^2 \mu \sim 1$ ; this is consistent with the requirement  $\mu^2 \Delta A_\perp \gg 1$  mentioned above (which sets the regime of applicability of the effective theory) at weak coupling:  $1/g^2 \gg 1$ .

---

<sup>1</sup> Beyond a perturbative treatment of the cubic Casimir one would have to add the quartic Casimir, too, so that the action is bounded from below [18].

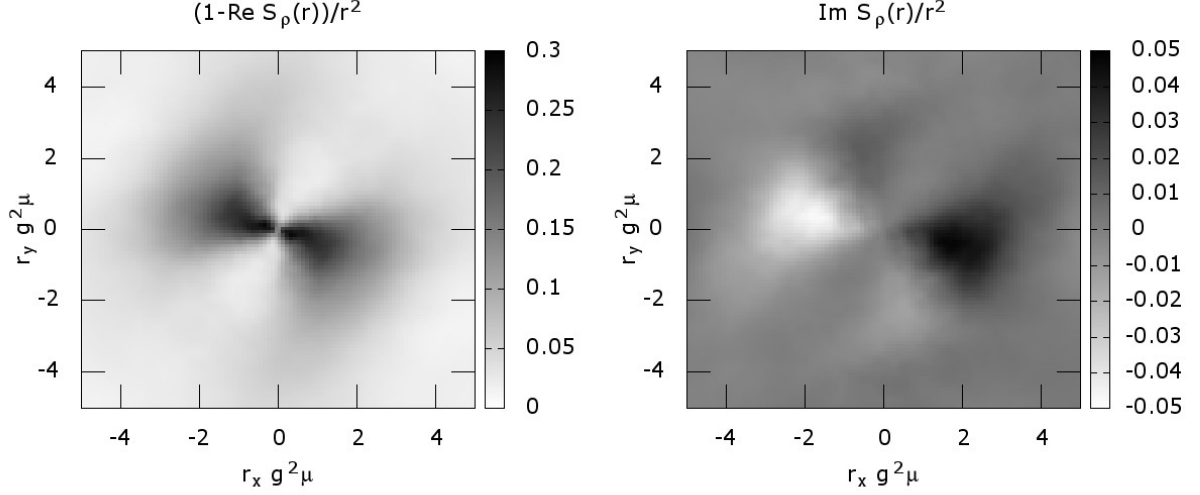


FIG. 1: The S-matrix in the fundamental representation as a function of the dipole vector  $\mathbf{r} = (r_x, r_y)$  at fixed impact parameter  $\mathbf{b} = 0$  for one particular random configuration of color charges  $\rho^a(\mathbf{x})$ .

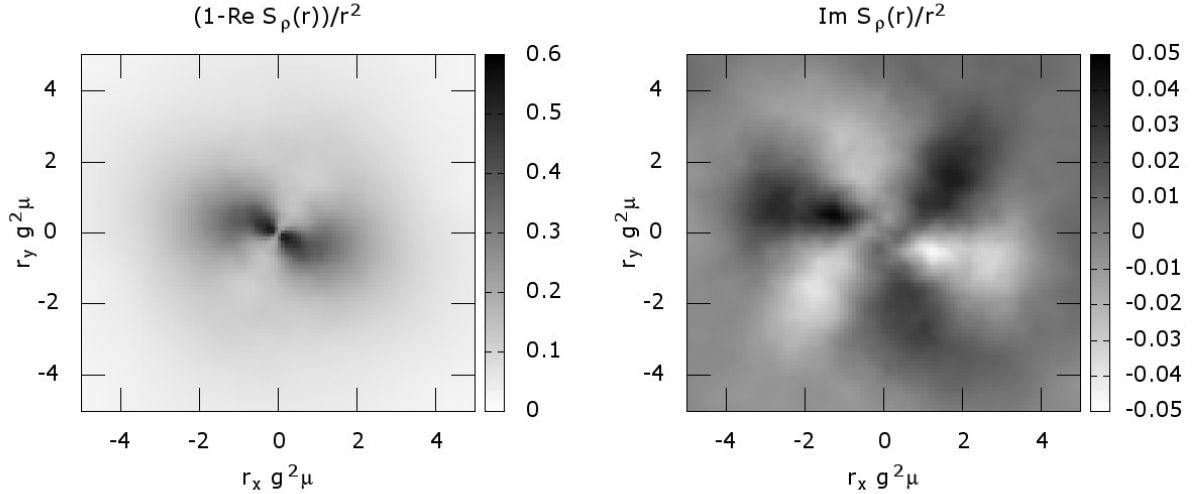


FIG. 2: Same as Fig. 1 for a second configuration of color charges  $\rho^a(\mathbf{x})$ .

Figure 3 shows our results for the averaged amplitudes of the first four azimuthal harmonics. As expected, the biggest one is the quadrupole amplitude  $\langle A_2 \rangle$  which reaches  $\gtrsim 20\%$  at  $r \lesssim 1/Q_s$ . Such values are in the range of the asymmetries extracted phenomenologically [7] for high-multiplicity p+Pb collisions at LHC energies. However, here we have not made any attempts to bias the configurations towards “high multiplicities”. The fact that the variance  $\sqrt{\langle (\delta A_2)^2 \rangle}$  is not much smaller than  $\langle A_2 \rangle$  indicates that some configurations generate much larger elliptic asymmetries than others. Also, we observe that  $\langle A_2 \rangle$  is approximately constant for  $r < 1/Q_s$  since up to quadratic order the real part of the S-matrix is

$$D(\mathbf{r}) = \frac{g^2}{2N_c} \text{tr}(\mathbf{r} \cdot \mathbf{E})^2 - \frac{1}{2} \frac{g^4}{4N_c^2} [\text{tr}(\mathbf{r} \cdot \mathbf{E})^2]^2 + \dots \quad (15)$$

at small  $r$ . To derive this expression one performs a gradient expansion of  $\text{Re tr } V(\mathbf{x})V^\dagger(\mathbf{y})$ , assuming that the electric field is smoothly varying over scales of order  $r$ . The leading term on the r.h.s., if scaled by  $1/r^2$ , is independent of  $r$  which is consistent with the observed constant  $\langle A_2 \rangle$  at small  $\mathbf{r}$ .

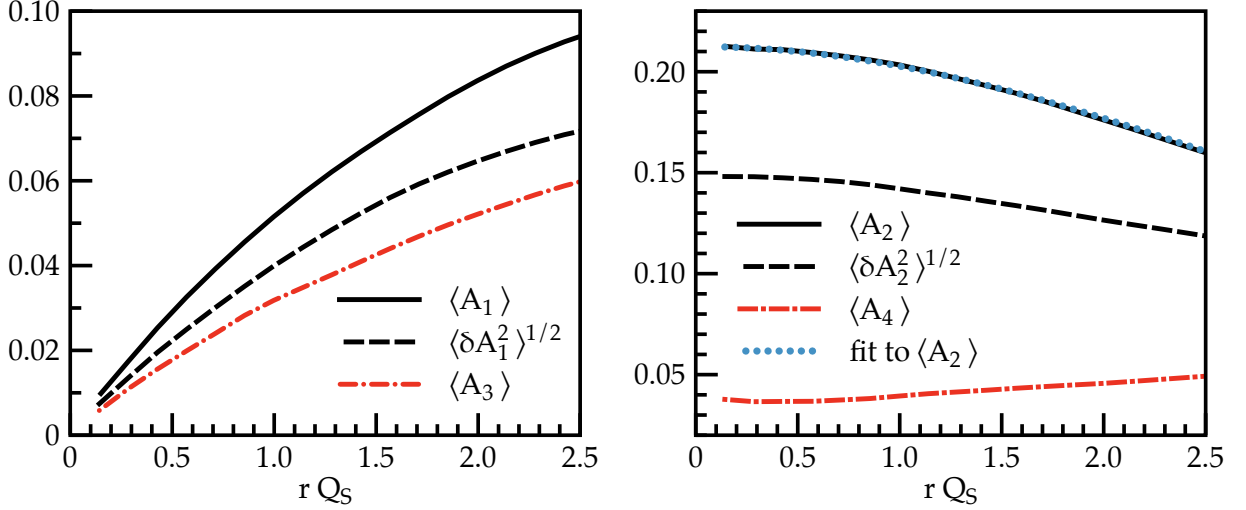


FIG. 3: The averaged amplitudes  $\langle A_n \rangle(r)$  vs. the dipole size  $r$  for  $n = 1, \dots, 4$ . The fit to  $\langle A_2 \rangle$  corresponds to the function from Eq. (16).

The numerical result for  $\langle A_2(r) \rangle$  agrees well with  $h_1^{\perp g}(x, r)$  derived in Ref. [16]:

$$h_1^{\perp g}(x, \mathbf{r}^2) \propto \frac{1}{r^2 Q_s^2} \left[ 1 - \exp\left(-\frac{r^2 Q_s^2}{4}\right) \right]. \quad (16)$$

The agreement suggests that (in the MV model)  $\langle A_2(r) \rangle$  essentially corresponds to the distribution of linearly polarized gluons, at least for sufficiently small dipoles. Below we shall see that the functions differ at large  $\mathbf{r}$ .

The second term in Eq. (15) generates a hexadecupole asymmetry at the next to leading order in  $r^2$ . However, the numerical result for  $A_4(r)$  shown in Fig. 3 is essentially constant at small  $r$ . We interpret this as due to corrections to the gradient expansion which leads to Eq. (15); a  $\sim \cos(4\phi)$  angular component appears already at  $\mathcal{O}(r^2)$  albeit with a much smaller amplitude than the  $\sim \cos(2\phi)$  harmonic.

We now turn to the odd amplitudes  $A_1$  and  $A_3$ . As already mentioned above, the expectation value of the odderon over a  $\mathcal{C}$ -even ensemble such as that generated by the action (1) is of course zero. Nevertheless, each particular configuration of semi-classical small- $x$  fields (2) *does* contain a  $\mathcal{C}$ -odd component and  $iO(\mathbf{r})$  as defined in Eq. (7) is non-zero. This is due to fluctuations of the saturation momentum  $Q_s$  in impact parameter space [19],

$$iO(\mathbf{r}) \sim i\alpha_s \mathbf{r} \cdot \nabla_{\mathbf{b}} (1 - D(\mathbf{r}, \mathbf{b})) \simeq i\alpha_s r^3 Q_s^2 Q_c \mathcal{B} \cos \phi_r \left[ 1 - \frac{r^2}{4} \left( \frac{Q_c^2 \cos^2 \phi_r}{3} + Q_s^2 \right) \right]. \quad (17)$$

The expression on the r.h.s. corresponds to an expansion in powers of  $r$ ;  $Q_c$  is a cutoff for the spectrum of fluctuations of  $Q_s(\mathbf{b})$  which was otherwise assumed to be scale invariant, and  $\mathcal{B}$  is their amplitude [7]. Eq. (17) shows that for small dipoles, after we divide by the isotropic normalization factor  $\mathcal{N}(r) \sim r^2$ , that we should expect  $A_1 \sim r$  as well as a smaller  $A_3 \sim r^3$ . The lattice results appear consistent with  $\langle A_1 \rangle \sim r$  at  $r \ll 1/Q_s$  but so is  $\langle A_3 \rangle$ , albeit with a smaller slope. Future simulations on larger lattices may be able to push to smaller  $r$ , and the analytical derivation of Eq. (17) based on a simple fluctuation spectrum could perhaps be refined as well.

Just as for the elliptic asymmetry we have also computed the standard deviation of the amplitude  $A_1$ . Again, we find that  $\sqrt{\langle (\delta A_1)^2 \rangle}$  is not much smaller than  $\langle A_1 \rangle$ , i.e. that some configurations generate much larger dipole asymmetries than others.

We have also analyzed the effect of “smearing” the impact parameter of the projectile over a region corresponding to its size [20]. If the  $\mathbf{E}$ -field anisotropy exhibits a non-zero correlation length in the impact parameter plane [6–8], specifically a correlation length that exceeds the size of the dipole, then the azimuthal moments should remain approximately the same.

Hence, we have also computed the azimuthal amplitudes  $A_n$  from “smeared” configurations:

$$\overline{D}_\rho(\mathbf{r}, \mathbf{b}) = \int \frac{d^2 \mathbf{b}'}{\pi r^2} \Theta(r - |\mathbf{b} - \mathbf{b}'|) D_\rho(\mathbf{r}, \mathbf{b}'), \quad (18)$$

and similarly for  $i\overline{O}_\rho(\mathbf{r}, \mathbf{b})$ . On the r.h.s. the points  $\mathbf{x} = \mathbf{b}' + \mathbf{r}/2$  and  $\mathbf{y} = \mathbf{b}' - \mathbf{r}/2$  are now determined by  $\mathbf{r}$  and  $\mathbf{b}'$ . Equation (18) averages the S-matrix over an area  $\pi r^2$ . The result is shown in Fig. 4 which can be compared to Fig. 3

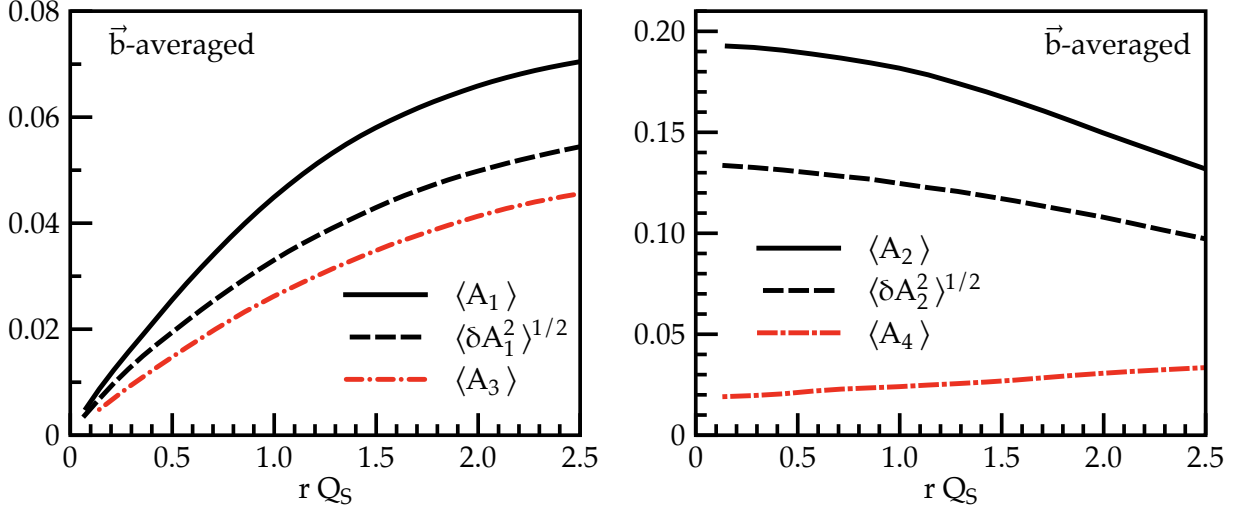


FIG. 4: Same as Fig. 3 (note modified scale on the vertical axes) for “smeared” S-matrix.

from above. Except for a slight suppression of their magnitudes, we do not observe any substantial modification of the amplitudes  $\langle A_n \rangle$ .

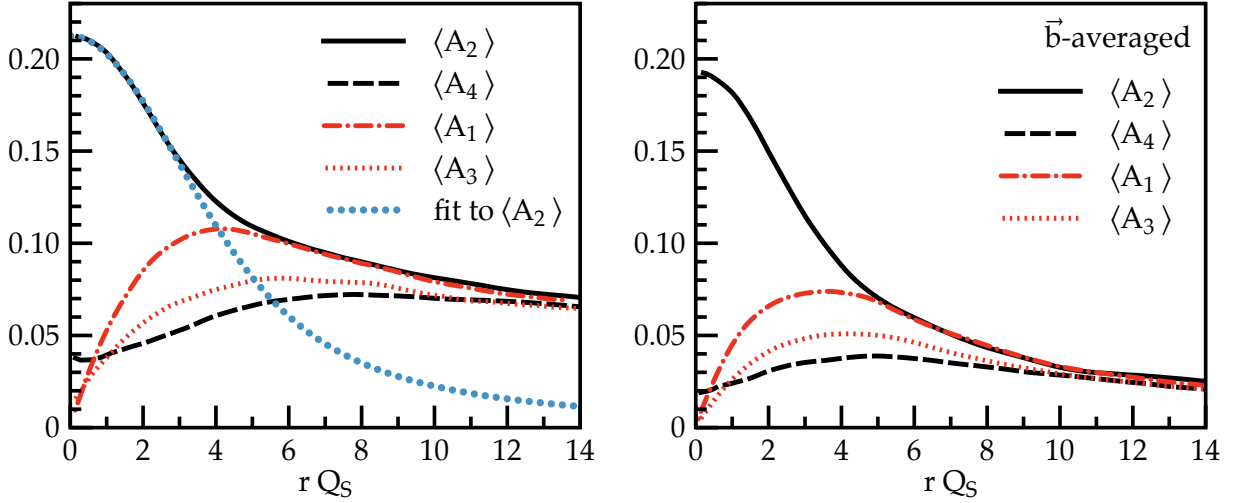


FIG. 5: The averaged amplitudes  $\langle A_n \rangle(r)$  vs. the dipole size  $r$  for  $n = 1, \dots, 4$ . This figure focuses on the behavior at large  $r \gg 1/Q_s$ . Left: fixed impact parameter  $\mathbf{b} = 0$ ; right: impact parameter averaged over an area  $\pi r^2$ .

The behavior for large dipoles is different, c.f. Fig. 5. For a fixed impact parameter the harmonic amplitudes approach a common non-zero function at large  $r \gg 1/Q_s$ . This is consistent with universal (angular) scale invariant fluctuations of the azimuthal dependence of the S-matrix. Indeed, if  $D(\mathbf{r}, \mathbf{b})$  and  $O(\mathbf{r}, \mathbf{b})$  are first averaged over an area  $\pi r^2$ , see Eq. (18), then the resulting  $\langle A_n \rangle$  are strongly suppressed. This shows that the direction of  $\mathbf{E}$  is not correlated over distances far beyond  $\sim 1/Q_s$ . Also, as already mentioned above, at large  $r$  the function  $\langle A_2 \rangle(r)$  is seen to differ from  $h_1^{\perp g}(x, \mathbf{r}^2)$ .

We should stress that the behavior of  $\langle A_n \rangle$  at  $r \gg 1/Q_s$  is shown only to reveal their expected universality due to scale invariant fluctuations (on a circle) within the model used here. The result applies in the regime far below the lattice IR cutoff scale  $L$  or whichever other IR cutoffs one may choose when implementing the theory. On the other hand, in practice  $Q_s$  is expected to be on the order of a few GeV only at current collider energies and so distances of order  $10/Q_s$  are not much shorter than the confinement scale. The MV model used here does not provide a controlled approximation to QCD near the confinement scale.

## V. HIGH-ENERGY EVOLUTION

In this section we consider effects due to resummation of boost-invariant quantum fluctuations of the fields. This is done through the so-called JIMWLK [21, 22] functional renormalization group evolution which resums observables to all orders in  $\alpha_s \log(1/x) = \alpha_s Y$ . Performing a step  $\Delta Y$  in rapidity opens phase space for radiation of gluons which modifies the classical action (1). This corresponds to a “random walk” in the space of Wilson lines  $V(\mathbf{x})$  [22–24]:

$$\partial_Y V(\mathbf{x}) = V(\mathbf{x}) \frac{i}{\pi} \int d^2 \mathbf{u} \frac{(\mathbf{x} - \mathbf{u})^i \eta^i(\mathbf{u})}{(\mathbf{x} - \mathbf{u})^2} - \frac{i}{\pi} \int d^2 \mathbf{v} V(\mathbf{v}) \frac{(\mathbf{x} - \mathbf{v})^i \eta^i(\mathbf{v})}{(\mathbf{x} - \mathbf{v})^2} V^\dagger(\mathbf{v}) V(\mathbf{x}) . \quad (19)$$

The Gaussian white noise  $\eta^i = \eta_a^i t^a$  satisfies  $\langle \eta_a^i(\mathbf{x}) \rangle = 0$  and

$$\langle \eta_a^i(\mathbf{x}) \eta_b^j(\mathbf{y}) \rangle = \alpha_s \delta^{ab} \delta_{ij} \delta^{(2)}(\mathbf{x} - \mathbf{y}) . \quad (20)$$

The “left-right symmetric” form of Eq. (19) was introduced in [24, 25]. We solve the random walk numerically assuming, for simplicity, a fixed but small coupling  $\alpha_s = 0.14$  so that the speed of evolution is not too rapid<sup>2</sup>. Once an ensemble of Wilson lines on the transverse lattice has been evolved to rapidity  $Y$ , we can again compute the dipole scattering amplitude  $\mathcal{S}_Y(\mathbf{r})$ , its azimuthal Fourier decomposition and the corresponding saturations scale  $Q_s(Y)$  using Eq. (12). We stress that even though we consider a target of infinite transverse extent, that the evolution equation is solved on a transverse lattice which does allow for impact parameter dependent fluctuations.

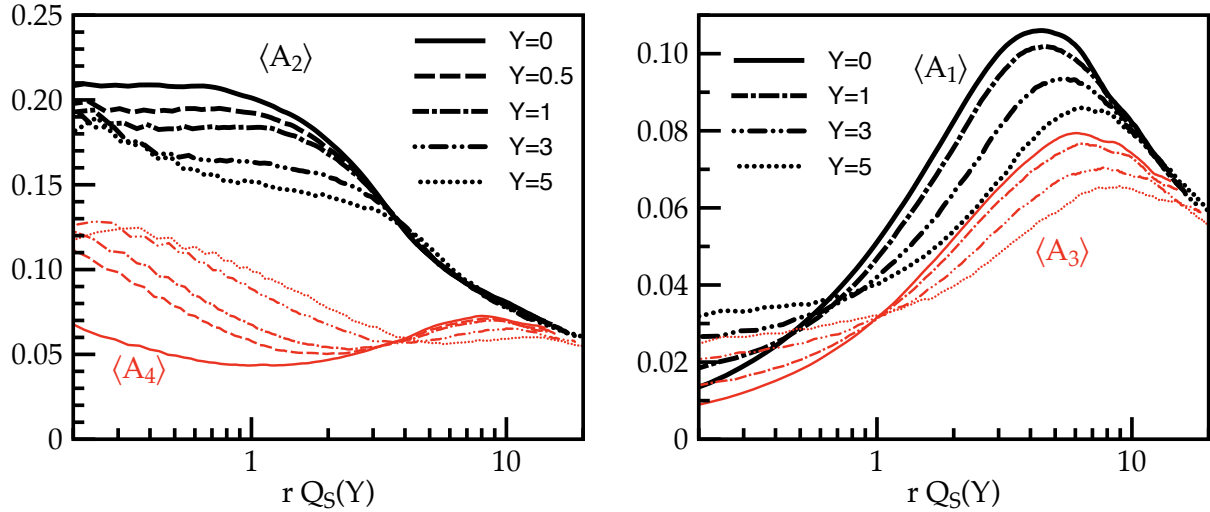


FIG. 6: JIMWLK evolution of  $\langle A_2 \rangle(r)$  and  $\langle A_4 \rangle(r)$  (left) resp. of  $\langle A_1 \rangle(r)$  and  $\langle A_3 \rangle(r)$  (right). In either plot the lower order harmonic corresponds to the upper set of curves.

In Fig. 6 (left) we show the evolution of  $\langle A_2 \rangle(r)$  and  $\langle A_4 \rangle(r)$ . Mean-field evolution of the dipole has been shown to wash out initial elliptic anisotropies rather quickly [6]. On the other hand, here we only observe a relatively slow decrease of  $\langle A_2 \rangle(r)$  with  $Y$ . This is rather intuitive since both the initial anisotropies at  $Y = 0$ , as well as those of the evolved JIMWLK configurations are generated by fluctuations of the “valence charges” in the transverse impact parameter plane. Furthermore, we observe that those harmonics which are small initially, i.e.  $\langle A_1 \rangle(r)$ ,  $\langle A_3 \rangle(r)$  and  $\langle A_4 \rangle(r)$ , in fact increase with rapidity at small  $r$ . There is again a universal behavior at very large  $r$ .

## VI. SUMMARY

Following the conjecture by Kovner and Lublinsky [6], we have analyzed azimuthal anisotropies of the S-matrix  $\mathcal{S}(\mathbf{r})$  for scattering of a dipole off a large nucleus. They arise due to fluctuations of the configuration of valence color charges  $\rho^a(\mathbf{x})$  in the transverse impact parameter plane<sup>3</sup>.

<sup>2</sup> The “time” variable for fixed coupling evolution is  $\alpha_s Y$ .

<sup>3</sup> An alternative picture in terms of  $\mathcal{O}(N_c^2)$  fluctuations of the energy-momentum tensor of a holographic shock wave has been discussed in Ref. [26]. Reference [27] considers the azimuthal structure of gluon bremsstrahlung off the fast beam-jet sources.

For a projectile in the fundamental representation of color SU(3) these fluctuations generate both charge conjugation even as well as odd configurations. For small dipoles,  $r \lesssim 1/Q_s$  the McLerran-Venugopalan [10] model gives  $\langle A_2 \rangle$  and  $\langle A_4 \rangle$  which are approximately constant ( $r$  independent). Also, the amplitude of the elliptic harmonic is much larger than that of the quadrangular harmonic,  $\langle A_2 \rangle \gg \langle A_4 \rangle$ . Odd harmonics appear at higher order in  $r$  [7, 19] and so their amplitudes decrease with decreasing  $r$ . The fluctuations of both  $A_1$  and  $A_2$  are comparable to their mean values, indicating that some configurations exhibit much larger anisotropies than others.

For large dipoles,  $r \gg 1/Q_s$ , we find that all amplitudes  $\langle A_1 \rangle(r), \dots, \langle A_4 \rangle(r)$  asymptotically approach a universal function if the S-matrix is evaluated at fixed impact parameter. This points at angular scale invariant fluctuations of the direction of  $\mathbf{E}$  over large distances. Accordingly, if the S-matrix is averaged over an area  $\pi r^2$  the resulting  $\cos(n\phi)$  amplitudes are strongly suppressed.

Impact parameter dependent fluctuations during QCD evolution in rapidity largely preserve the azimuthal amplitudes. Our calculations confirm that individual small- $x$  target field configurations do exhibit angular dependence which would play an important role in understanding azimuthal  $v_n$  harmonics in pp and pA collisions [6–8]. In particular, the amplitude of elliptic anisotropies  $\langle A_2 \rangle \sim 15 - 20\%$  is on the order of the  $v_2$  harmonic observed in p+Pb collisions at the LHC. Moreover, similar studies as the one performed here might be able to shed some light on the behavior of the linearly polarized gluon distribution  $h_1^{\perp g}(x, \mathbf{r}^2)$  at small  $x$ ; work in that direction is in progress.

### Acknowledgments

We thank B. Schenke, S. Schlichting and L. McLerran for useful discussions. A.D. gratefully acknowledges support by the DOE Office of Nuclear Physics through Grant No. DE-FG02-09ER41620 and from The City University of New York through the PSC-CUNY Research Award Program, grant 67119-0045. V.S. thanks D. Shubina for discussions and for providing a C++ library for color matrices. The numerical computations were performed at the High Performance Computing Center, Michigan State University.

- 
- [1] B. Abelev *et al.* [ALICE Collaboration], Phys. Lett. B **719**, 29 (2013); Phys. Rev. C **90**, 054901 (2014).
  - [2] G. Aad *et al.* [ATLAS Collaboration], Phys. Rev. Lett. **110**, 182302 (2013); Phys. Lett. B **725**, 60 (2013); The ATLAS collaboration, ATLAS-CONF-2014-021.
  - [3] S. Chatrchyan *et al.* [CMS Collaboration], Phys. Lett. B **718**, 795 (2013); Phys. Lett. B **724**, 213 (2013).
  - [4] A. Adare *et al.* [PHENIX Collaboration], Phys. Rev. Lett. **111**, 212301 (2013); A. Adare *et al.* [PHENIX Collaboration], arXiv:1404.7461 [nucl-ex].
  - [5] Li Yi for the STAR Collaboration, arXiv:1410.1978 [nucl-ex].
  - [6] A. Kovner and M. Lublinsky, Phys. Rev. D **83**, 034017 (2011); Phys. Rev. D **84**, 094011 (2011); Int. J. Mod. Phys. E **22**, 1330001 (2013).
  - [7] A. Dumitru and A. V. Giannini, arXiv:1406.5781 [hep-ph] (Nucl. Phys. A, in print).
  - [8] A. Dumitru, L. McLerran and V. Skokov, arXiv:1410.4844 [hep-ph].
  - [9] S. Schlichting and B. Schenke, Phys. Lett. B **739**, 313 (2014).
  - [10] L. D. McLerran and R. Venugopalan, Phys. Rev. D **49**, 2233 (1994); Phys. Rev. D **49**, 3352 (1994); Y. V. Kovchegov, Phys. Rev. D **54**, 5463 (1996).
  - [11] A. Krasnitz and R. Venugopalan, Nucl. Phys. B **557**, 237 (1999).
  - [12] T. Lappi, Eur. Phys. J. C **55**, 285 (2008).
  - [13] J. Jalilian-Marian, A. Kovner, L. D. McLerran and H. Weigert, Phys. Rev. D **55**, 5414 (1997).
  - [14] Y. Hatta, E. Iancu, K. Itakura and L. McLerran, Nucl. Phys. A **760**, 172 (2005).
  - [15] P. J. Mulders and J. Rodrigues, Phys. Rev. D **63**, 094021 (2001); S. Meissner, A. Metz and K. Goeke, Phys. Rev. D **76**, 034002 (2007); F. Dominguez, J. W. Qiu, B. W. Xiao and F. Yuan, Phys. Rev. D **85**, 045003 (2012).
  - [16] A. Metz and J. Zhou, Phys. Rev. D **84**, 051503 (2011).
  - [17] S. Jeon and R. Venugopalan, Phys. Rev. D **70**, 105012 (2004); Phys. Rev. D **71**, 125003 (2005).
  - [18] A. Dumitru, J. Jalilian-Marian and E. Petreska, Phys. Rev. D **84**, 014018 (2011); A. Dumitru and E. Petreska, Nucl. Phys. A **879**, 59 (2012).
  - [19] Y. V. Kovchegov and M. D. Sievert, Phys. Rev. D **86**, 034028 (2012) [Erratum-ibid. D **86**, 079906 (2012)].
  - [20] B. Schenke, S. Schlichting, and R. Venugopalan: priv. comm.; T. Lappi, arXiv:1501.05505 [hep-ph].
  - [21] J. Jalilian-Marian, A. Kovner, A. Leonidov and H. Weigert, Nucl. Phys. B **504**, 415 (1997); Phys. Rev. D **59**, 014014 (1998); J. Jalilian-Marian, A. Kovner and H. Weigert, Phys. Rev. D **59**, 014015 (1998); J. Jalilian-Marian, A. Kovner, A. Leonidov and H. Weigert, Phys. Rev. D **59**, 034007 (1999) [Erratum-ibid. D **59**, 099903 (1999)]; E. Iancu, A. Leonidov and L. D. McLerran, Nucl. Phys. A **692**, 583 (2001); E. Iancu and L. D. McLerran, Phys. Lett. B **510**, 145 (2001); E. Ferreira, E. Iancu, A. Leonidov and L. McLerran, Nucl. Phys. A **703**, 489 (2002); E. Iancu, A. Leonidov and L. D. McLerran, Phys. Lett. B **510**, 133 (2001).



- [22] H. Weigert, Nucl. Phys. A **703**, 823 (2002); A. H. Mueller, Phys. Lett. B **523**, 243 (2001).
- [23] J. P. Blaizot, E. Iancu and H. Weigert, Nucl. Phys. A **713**, 441 (2003).
- [24] T. Lappi and H. Mäntysaari, Eur. Phys. J. C **73**, 2307 (2013).
- [25] A. Kovner and M. Lublinsky, JHEP **0503**, 001 (2005).
- [26] J. Noronha and A. Dumitru, Phys. Rev. D **89**, 094008 (2014).
- [27] M. Gyulassy, P. Levai, I. Vitev and T. S. Biro, Phys. Rev. D **90**, no. 5, 054025 (2014).